Development of a Variable Conductance Cold Plate for Spatial and Temporal Isothermality Across Power Scales

Elizabeth K. Seber[1] and Michael C. Ellis[2]
Advanced Cooling Technologies, Inc. Lancaster, PA 17601

For low earth orbiting satellites, environmental conditions rapidly change throughout a single orbit. These changes affect the radiative heat sink of these satellites, and in turn, rapidly alter the temperatures of sensitive onboard instrumentation. As such, there exists a need for a thermal control system to maintain such instrumentation at a uniform and consistent temperature despite environmental changes. Such a thermal system must also be low in size, weight, and power if it is to be adopted into LEO satellites. Through a NASA Phase II SBIR, ACT has developed such a thermal system, consisting of a variable conductance cold plate (VCCP) to provide spatial and temporal isothermality to mounted electronic components. The technology builds on ACT's experience with passive two-phase devices, specifically variable conductance heat pipes (VCHP) and vapor chambers, which address spatial isothermality. Temporal isothermality is handled by the VCHPs, which are charged with a working fluid at saturation conditions and a non-condensable gas (NCG). During operation, vapor that is generated from the VCHP's evaporator moves to the condenser. As the heat load/sink temperature changes, the working fluid seeks to operate at a higher temperature. This increases pressure as the working fluid exists at saturation conditions. This increase pushes back the NCG and opens more condensing areas. As the opposite occurs, NCG pushes forward and blankets a portion of the condensing area of the VCHP. As the condenser surface area changes, the conductance of the heat pipe varies, which allows the VCHP to carry heat at a higher rate and mitigate the effects of heat load or sink temperature changes. ACT has tested two subscale versions for different power levels, charged with either acetone or ammonia and expanded this technology to a cold plate boasting a heat collection surface area of 0.5 m^2.

Nomenclature

CCHP	=	Constant Conductance Heat Pipe
DMLS	=	Direct Metal Laser Sintering
LEO	=	Low Earth Orbit
n	=	Number of Moles
NCG	=	Non-Condensable Gas
P	=	Pressure
$P_{Partial}$	=	Partial Pressure
R	=	Ideal Gas Constant
T	=	Temperature
T_{Sink}	=	Sink/Coolant Temperature
T_{Vapor}	=	Vapor Temperature
V	=	Volume
VCCP	=	Variable Conductance Cold Plate
VCHP	=	Variable Conductance Heat Pipe

I. Introduction

THERMAL management systems for satellites must be capable of heat removal despite the harsh and changing environmental conditions experienced in orbit, all while trying to maintain low size, weight, and power (SWaP) in a volume-critical and power-limited vehicle. As such, two-phase systems prove to be superior compared to single-

[1] R&D Engineer II, R&D, 1046 New Holland Avenue, Lancaster, PA 17601, USA.
[2] Senior Engineer, R&D, 1046 New Holland Avenue, Lancaster, PA 17601, USA.

phase systems in that they offer the removal of significant heat loads, enhanced heat transfer, and temperature uniformity all while maintaining reduced mass, volume, and power usage. For such space applications, ACT has developed a variable conductance cold plate (VCCP) which boasts not only the spatial isothermality typically achieved by two-phase systems, but also temporal isothermality to counteract the rapidly changing environmental conditions experienced by satellites in orbit.

The VCCP is comprised of three main technologies: a vapor chamber, variable conductance heat pipes (VCHPs), and a two-phase heat exchanger, as shown in Figure 1. Heat sources, such as power-dense electronics, are mounted to the heat collection surface area of the vapor chamber. Working fluid within the vapor chamber exists at saturation, with liquid occupying wick structures that line the vapor chamber and vapor occupying the remaining space. Due to this working fluid operating at saturation, and since the heat is transported as latent heat, the heat collection surface sees a spatially uniform temperature. As heat enters the system, vapor is generated off the heat collection surface, where it then condensates onto the exterior faces of the VCHPs. The wick structure then transports the liquid back up to the heat collection surface, where the process repeats. In this way, the vapor chamber can remove non-uniform heat loads from across the heat collection surface.

The temporal isothermality of the system is then addressed by the next component of the system, the variable conductance heat pipes. These heat pipes are charged with a working fluid at saturation conditions, as well as a non-condensable gas (NCG). As heat is applied to the evaporator portion of the VCHPs, vapor is generated and moves to the condenser portion of the VCHP. Here, liquid forms as the vapor condenses, and is returned to the evaporator portion through wicked structures, in a manner similar to the operation of the vapor chamber. However, the addition of the NCG provides some variability to this performance. As the vapor pushes from the evaporator to the condenser, it continuously pushes the NCG to the far end, forming a pocket of NCG known as the NCG reservoir. As conditions such as the heat load or sink temperature change, the volume of the NCG reservoir also changes. This covers a portion of the condenser portion of the VCHP, altering the effective conductance of the VCHP.

The heat transported by the VCHPs is finally removed using a two-phase heat exchanger, transporting the heat from the system, and transporting it to the ultimate heat sink. In low-earth orbit applications, this heat exchanger may be replaced by a radiator panel. To maintain control over the sink temperature, ACT chose to use a fin-tube heat exchanger as the two-phase heat exchange, where the tubes are the condensing section of the VCHPs, and a coolant is pumped in crossflow to fins and tubes. By combining these three technologies, the VCCP can provide spatial and temporal isothermality over a large surface area while maintaining a compact, low-mass, and low-power thermal management system.

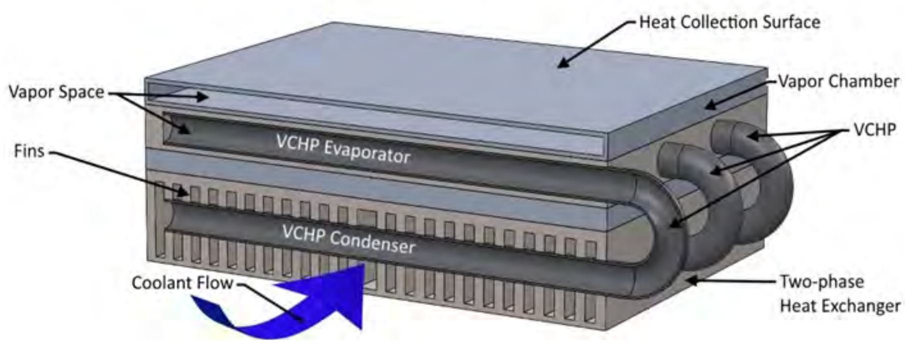

Figure 1. Cold Plate Concept (Components Shown Oversized to Aid Visualization).

ACT has previously designed, fabricated, and tested a variable conductance cold plate (VCCP) that is capable of significant power rejection while maintaining low spatial and temporal temperature deviation. This was done through a subscale prototype, and since the findings of this were published [1], ACT has developed two more VCCPs with different working fluids and power loads. The differences in the development of these VCCPs scales are presented here to demonstrate the performance across power scales.

II. Analytical Model and Design Across Scales

A. Methodology

Using an in-house system model, ACT has analytically modeled the design and performance of three unique variable conductance cold plates; the key differences between these models are shown in Table 1. The developed model first individually models the vapor chamber, the VCHPs, and the heat exchanger. The model then integrates these three major components to model the thermal performance across a single VCHP. The model then combines multiple VCHP units to model the whole cold plate.

Table 1. Key Properties of the Three Different VCCP Models

Model Name	Working Fluid	Max Power Load (W)	Heat Collection Surface Area (m^2)
Subscale Acetone	Acetone	210	0.035
Subscale Ammonia	Ammonia	250	0.055
Full-Scale	Acetone	500	0.5

The methodology for this analytical model is described in greater detail in a previous ICES paper (ICES-2021-354) [1], however, the process is summarized here for completeness. Starting with the heat rejection end of the system, which is the heat exchanger and where conditions are predefined, a thermal resistance network is used to determine the temperature of the vapor within the condensing portion of the heat pipe. Given that the conditions within the heat pipe are at saturation, the vapor temperature throughout the heat pipe is assumed uniform for this model. A second thermal resistance network connecting the vapor within the evaporation portion of the heat pipe and the heat collection surface is then used to determine the temperature at the heat collection surface. With this model, we can plot how the heat collection surface temperature changes as the sink conditions (such as sink temperature or coolant flow rate) change.

In the case of a model which uses constant conductance heat pipes (CCHP), this would be the end of the modeling process. To now demonstrate a variable conductance heat pipe (VCHP) within the model, a relationship between the non-condensable gas (NCG) and vapor must be established. The balance between the vapor and NCG determines the length of the heat pipe condenser blanketed by the NCG, which can be considered as an inactive section of the heat pipe as it is not actively contributing to the heat transfer path. This change in active versus inactive condenser length alters the thermal resistance through this portion, and so this length must be calculated. The ideal gas law (Eqn. 1) relates the volume of the NCG (which is the inactive volume of the heat pipe's condensing section) with the partial pressure of the gas and the temperature of the sink. The partial pressure itself is a function of the vapor temperature within the heat pipe. Knowing the inactive volume allows us to determine the active length of the condenser to use for the earlier thermal resistance calculations.

Given that the number of moles of NCG in the system is constant across all conditions, we can form a function that uses the heat pipe vapor temperature, the sink temperature, and the heat loads as inputs (Eqn. 2). This function can be formulated such that it is the difference between the number of moles at a max vapor temperature (when the inactive length is at its smallest) and at an arbitrary vapor temperature (which is the value we are seeking to derive). Since this equation must always equate to zero (as the number of moles cannot change), the root of this function results in the more accurate vapor temperature of the VCHPs as the inputs to the system change. This new vapor temperature can now be used with the pre-established thermal resistance networks to complete the model.

$$n = \frac{P_{Partial} \times V_{Inactive}}{R \times T_{Sink}} \tag{1}$$

$$F\left(T_{Sink}, T_{Vapor}, Heat\ Load\right) = n\left(T_{Vapor\ Max}\right) - n\left(T_{Vapor}\right) \tag{2}$$

B. Analytical Model Results

The key parameters of the analytical model were altered to reflect the differences between the three models. From there, additional parameters were altered and noted in a design study to optimize the three different prototypes. These parameters about which the models were optimized include the number of heat pipes, the diameter of heat pipes, and the volume of the NCG reservoir. In optimizing these models, parameters were selected based on the maximum temperature shown by the heat collection surface, and the rate of temperature change for the heat collection surface based on the rate of sink temperature change.

1. Subscale Acetone VCCP Model Results

For the initial subscale prototype, it was determined that the minimal amount of heat pipes necessary to demonstrate the performance would be acceptable. This number of heat pipes was determined to be three pipes. Using the analytical model described in Section II. Analytical Model and Design Across Scales A. Methodology, ACT began a parametric optimization study by varying the diameter of the heat pipes within this model. Other parameters which could have been varied were held constant and are described in Table 2. The NCG Reservoir Volume was held constant at 1 cm^3 while the heat pipe diameters were varied, and the results of this parametric study are shown in Figure 2. While 0.375-inch diameter heat pipe resulted in the hottest temperatures experienced by the heat collection surface area, it also resulted in the lowest temperature change across the range of coolant temperatures. The temperature of the heat collection surface area decreases with increasing heat pipe size due to the increased condensing surface area presented by the larger heat pipes. However, as heat pipe size decreases, the VCHP demonstrates improved temporal isothermality as the NCG can cover the condensing area quicker due to the smaller cross-sectional area. Since our goal with the VCHPs is to increase the temporal isothermality, we selected 0.375-inch diameter heat pipes for the Subscale Acetone VCCP. Using 0.375-inch diameter heat pipes within the analytical model, the NCG reservoir volumes were then varied. The results of this are shown in Figure 3. ACT selected an NCG reservoir size of 4 cm^3 to move forward with, as again it showed to have the lowest temperature change across the range of coolant temperatures when compared to smaller reservoir sizes, demonstrating improved temporal isothermality.

Table 2. Parameters Held Constant for Optimizing the Subscale Acetone VCCP

Parameter	Value
Cold Plate Length	6 in.
Cold Plate Width (Heat Pipe Evaporator Length)	9 in.
Heat Exchanger Length (Heat Pipe Condenser Length)	8 in.
Number of Heat Pipes	3
Heat Load	210 W
Coolant Flow Rate	2 L/min
Working Fluid:	Acetone

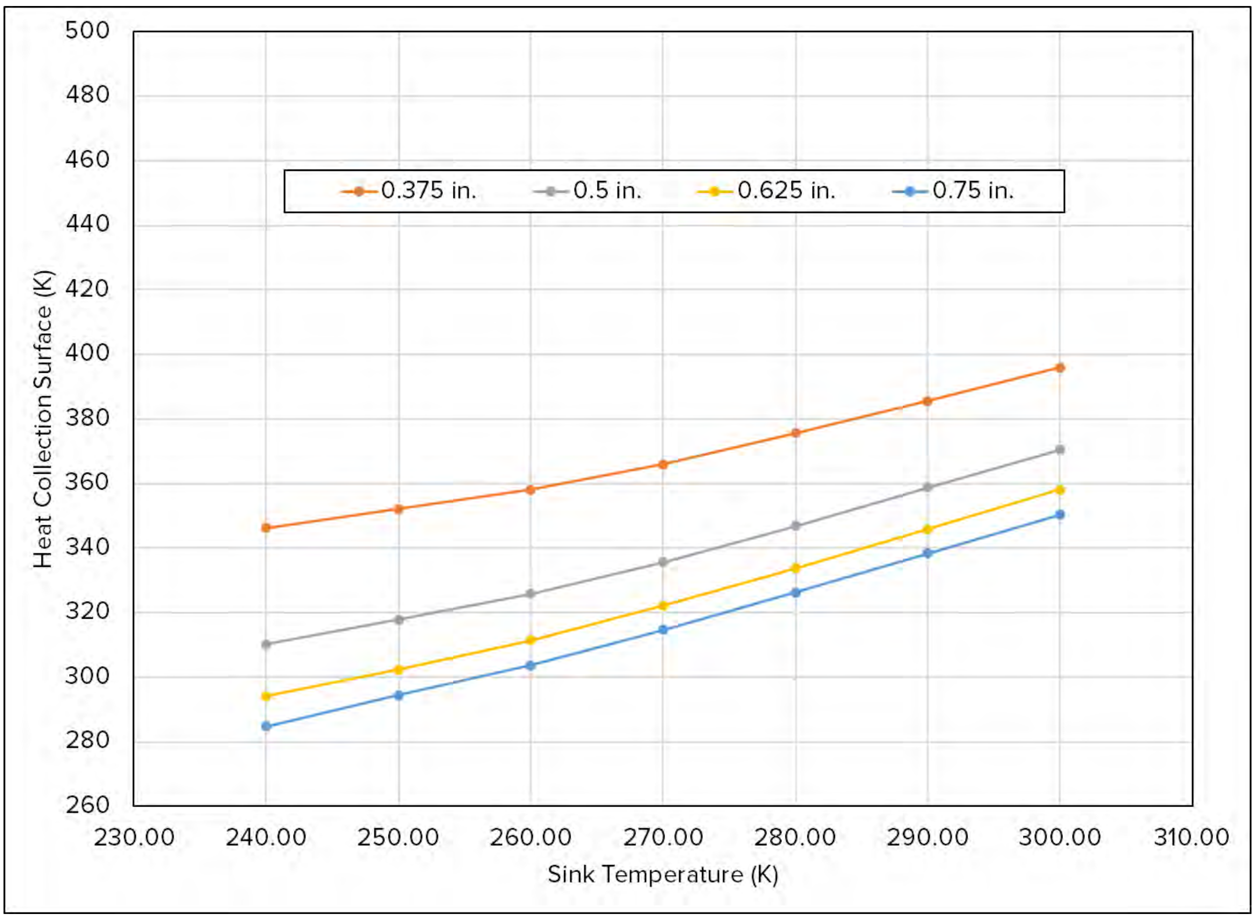

Figure 2. Subscale Acetone VCCP - Optimization Study for Heat Pipe Diameters; Heat Collection Surface Temperature vs. Coolant Temperature. Heat Load for all cases was 210 W. Reservoir size was set to 1 cm^3.

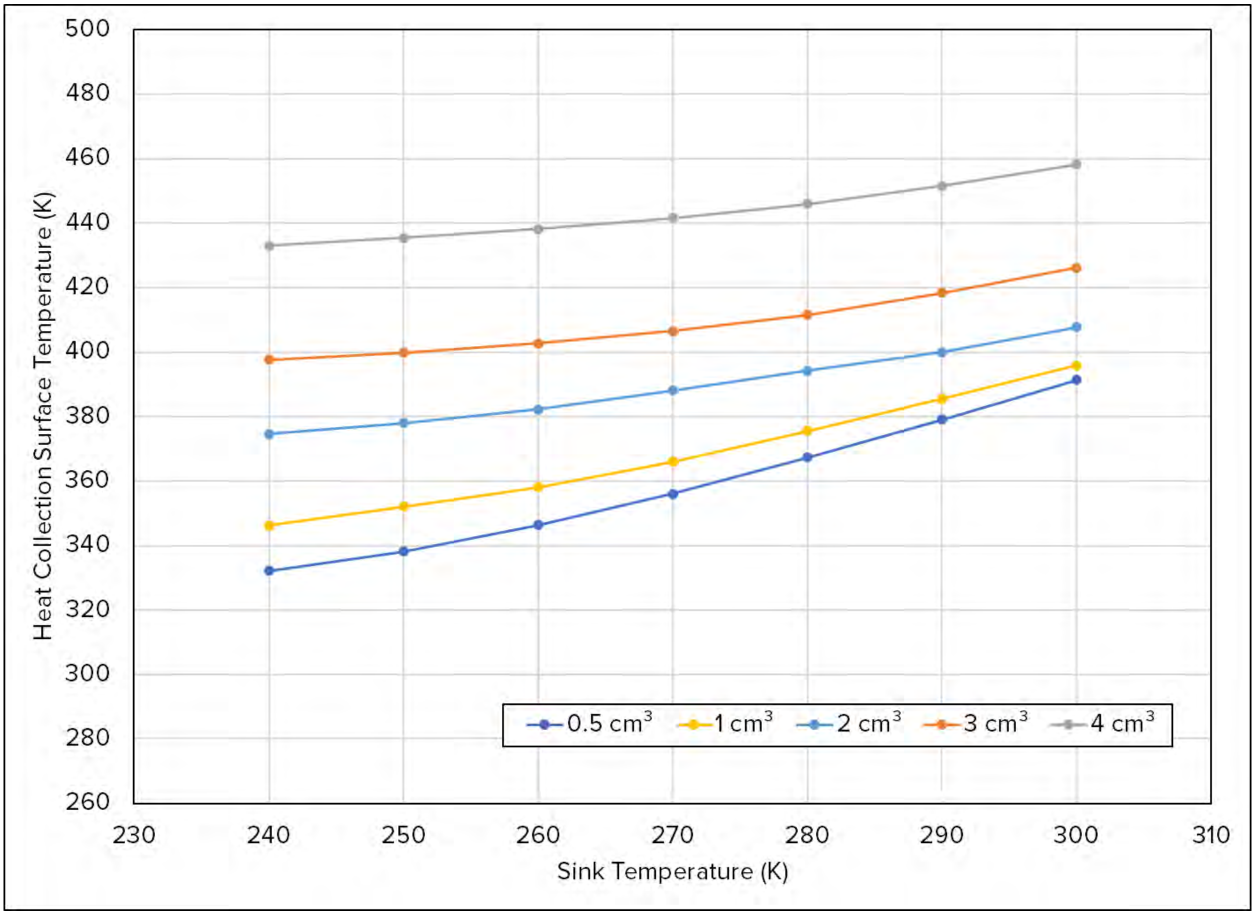

Figure 3. Subscale Acetone VCCP – Optimization Study for NCG Reservoir Volume; Heat Collection Surface Temperature vs. Coolant Temperature. Heat Load for all cases was 210 W. Heat Pipe Diameter was set to 0.375 in.

2. Subscale Ammonia VCCP Model Results

The first optimization study for the Subscale Ammonia VCCP investigated the effects of the heat pipe diameter size on the performance of the VCCP and is shown in Figure 4. At the time of this optimization study, the heat load for this model had not yet been determined, so the attached results also explore the performance of the VCCP across heat loads. From this graph, assuming the coolant changes temperature at a rate of 1 K/min, at the low end a VCCP with 0.25in diameter heat pipes carrying 1500 W sees a heat collection surface temperature change rate of 0.26 K/min. At the high end, a VCCP with 0.50-in-diameter heat pipes carrying 500 W sees a heat collection surface temperature change of 0.57 K/min. ACT selected 0.50-in-diameter heat pipes for the Subscale Ammonia VCCP. The next optimization study investigated the effects of varying the NCG reservoir volume which is shown in Figure 5.

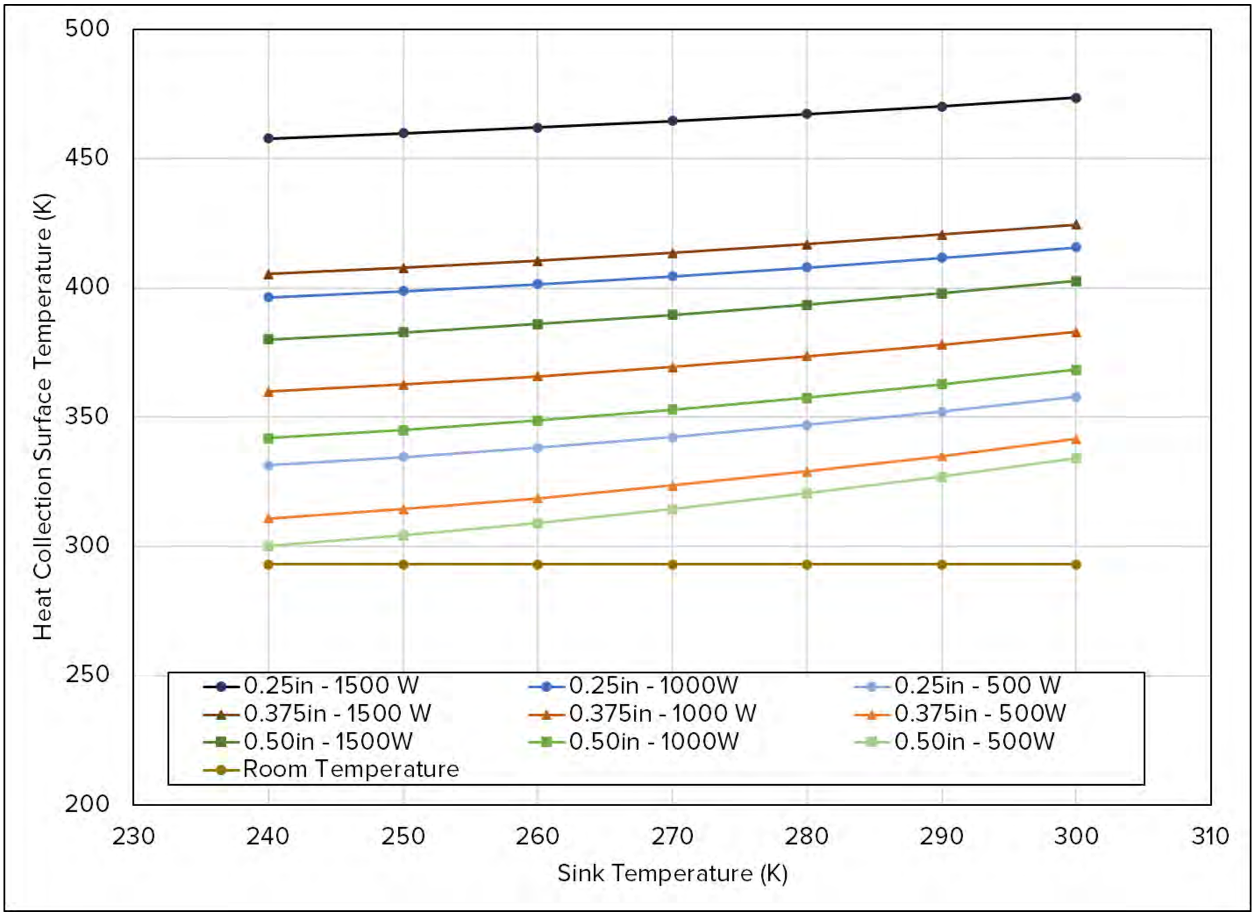

Figure 4. Subscale Ammonia VCCP - Optimization Study for Heat Pipe Diameters and Heat Loads; Heat Collection Surface Temperature vs. Coolant Temperature.

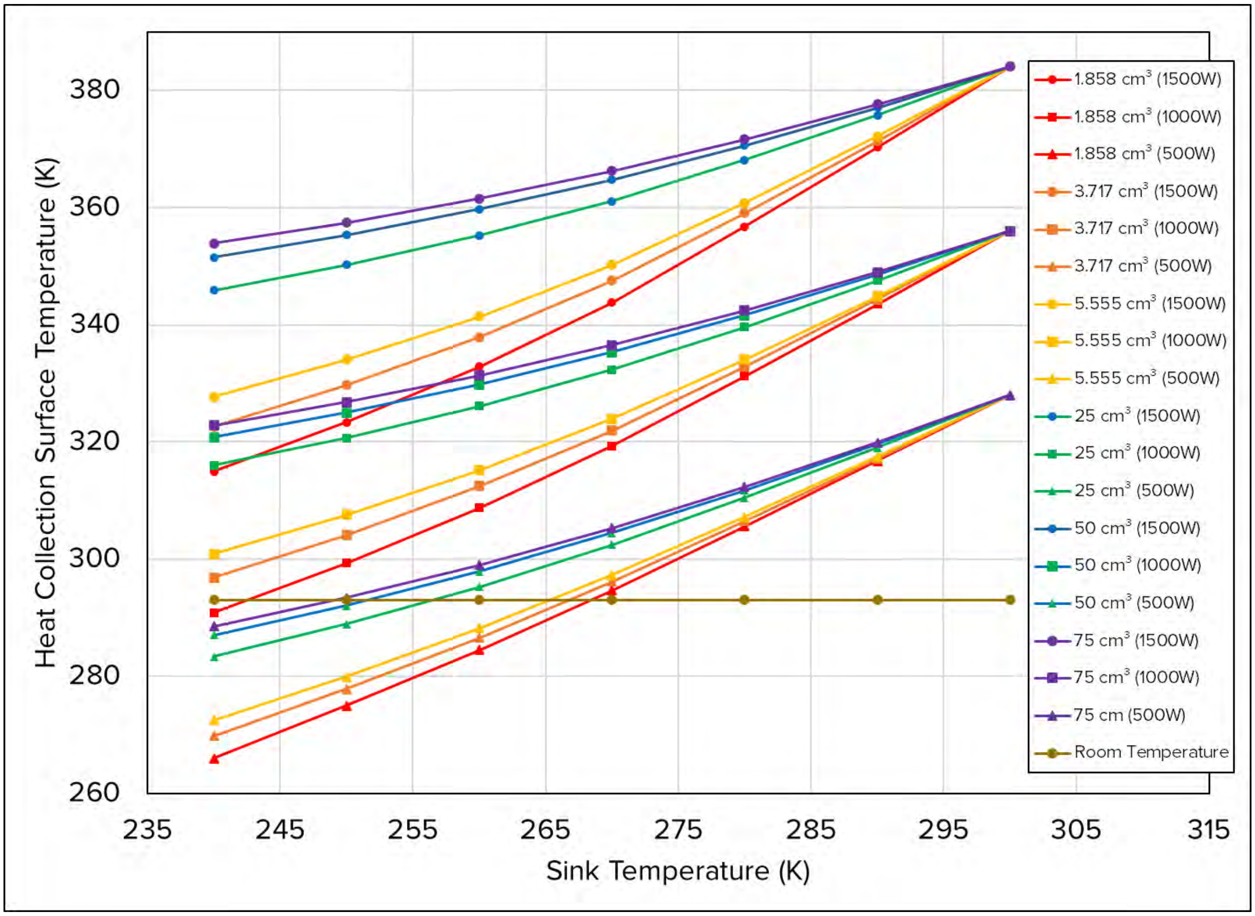

Figure 5. Subscale Ammonia VCCP – Optimization Study for NCG Reservoir Volume; Heat Collection Surface Temperature vs. Coolant Temperature.

3. Full-Scale VCCP Model Results

Following the optimization study completed for the previous two models, the Full-Scale VCCP Model was optimized for its heat pipe diameter (Figure 6) and NCG Reservoir volume (Figure 7). ACT selected 0.375-inch diameter heat pipes as they provided the best balance between lowered surface temperatures and lowered temperature gradient as coolant temperatures change. Additionally, this heat pipe size was selected for the Subscale Acetone VCCP and would provide an interesting comparison in heat pipe performance for the Full-Scale VCCP. For the full-scale model, ACT selected the NCG reservoir volume of 5.415 cm³. This reservoir volume equates to roughly ¼ of the available condensing length and is a balance of providing both lowered temperatures and a slower rate of change of temperature.

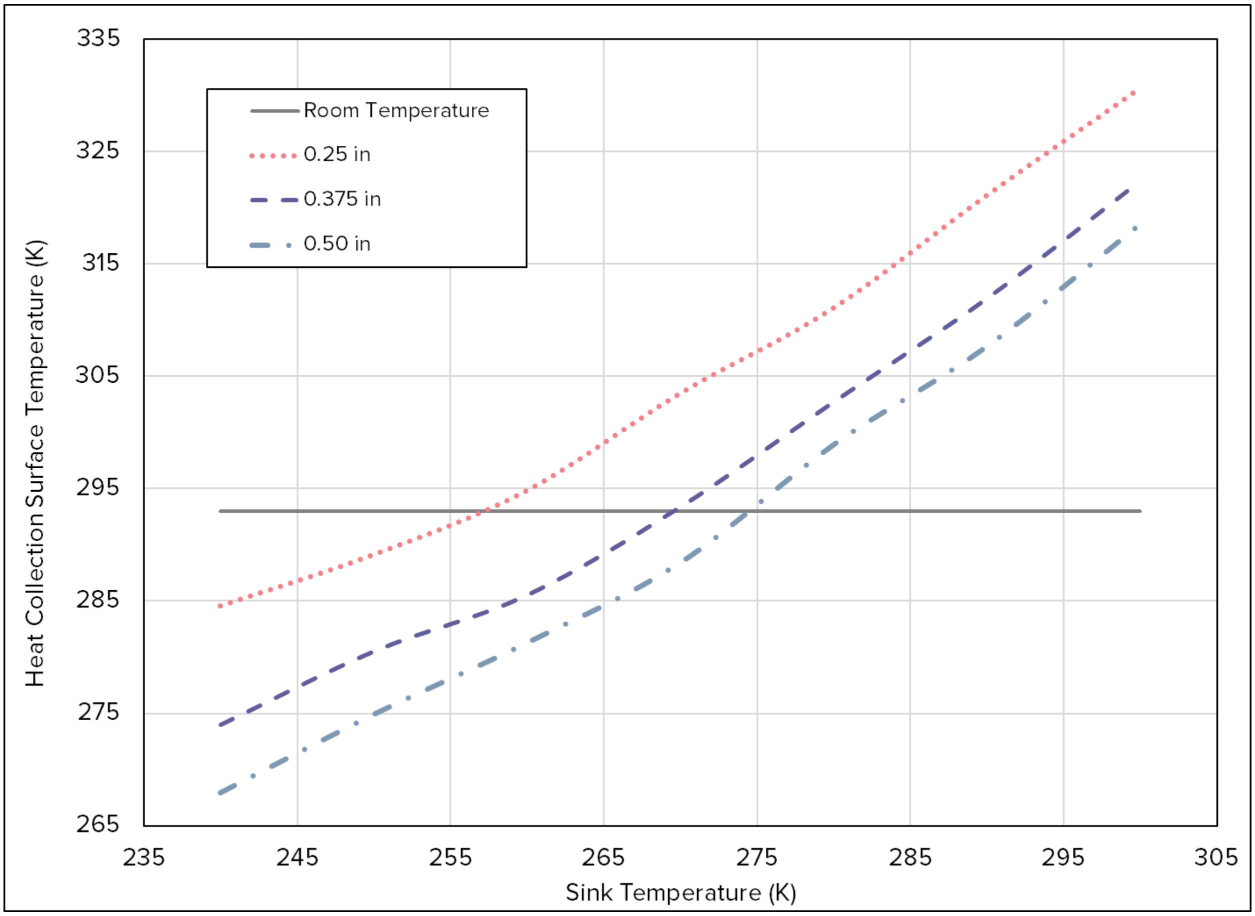

Figure 6. Full-Scale VCCP - Optimization Study for Heat Pipe Diameter; Heat Collection Surface Temperature vs. Coolant Temperature. Heat load is 500 w for all cases; reservoir volume set to ¼ of available condensing volume.

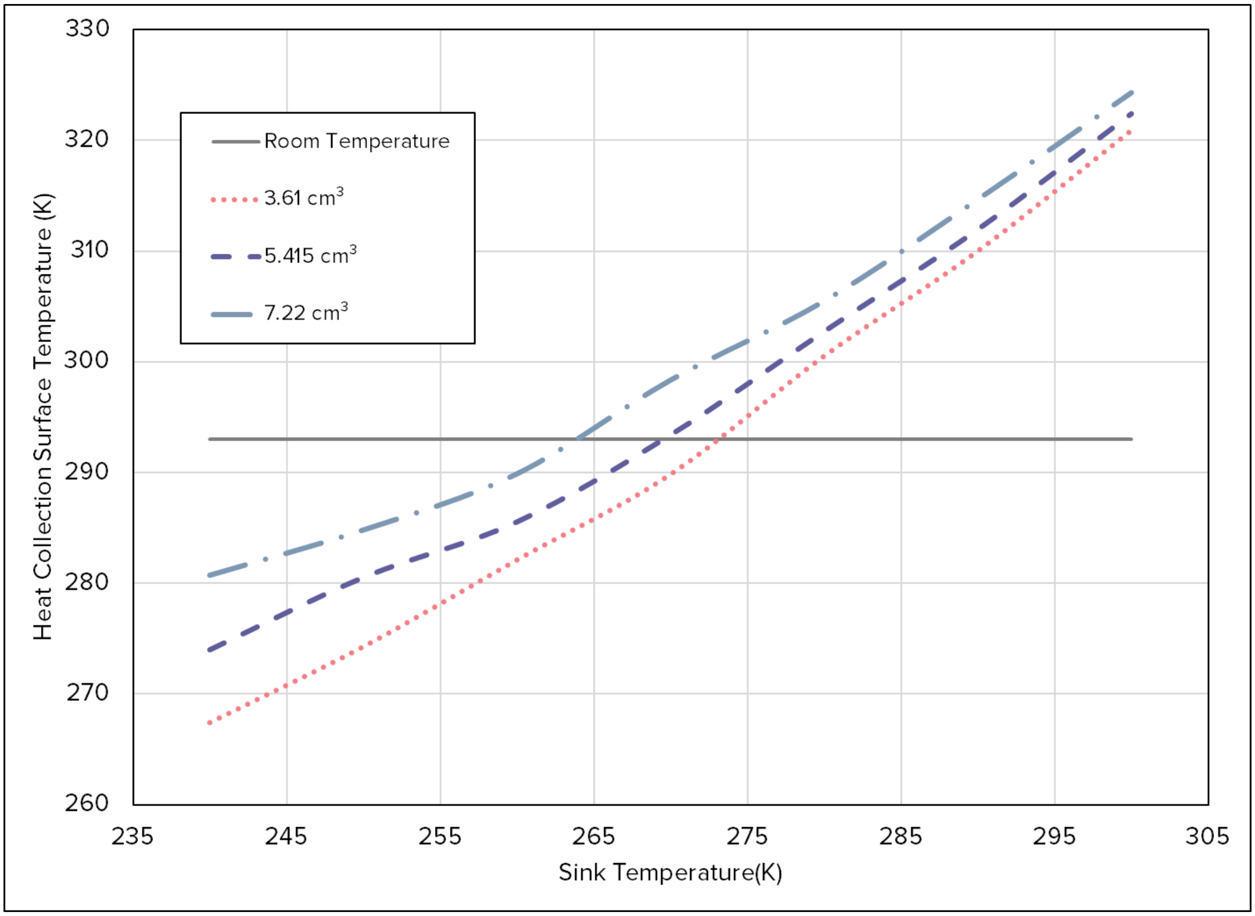

Figure 7. Full-Scale VCCP - Optimization Study for NCG Reservoir Volume; Heat Collection Surface Temperature vs. Coolant Temperature. Head Load is 500 W for all cases; Heat Pipe Diameter set to 0.375 in.

III. Testing and Results

A. Fabricated Prototypes

After optimizing each of the models designs through the analytical model, ACT designed and fabricated each version into a functional prototype. These prototypes were fabricated through both additive manufacturing and traditional manufacturing means.

1. Subscale Acetone VCCP Fabrication

The Subscale Acetone VCCP was fabricated through direct metal laser sintering (DMLS) out of the aluminum alloy AlSi10MG. Both the Vapor Chamber and Heat Exchanger were additively manufactured separately, with their respective portions of the heat pipes embedded within. Aluminum tubes were then used to connect the two components, and additional tubes were also added as fill tubes for both the vapor chamber and the heat pipes. The aluminum mesh was inserted into the heat pipes to act as the internal wick structure. The vapor chamber of this prototype was charged with acetone, and the heat pipes were charged with both acetone and argon.

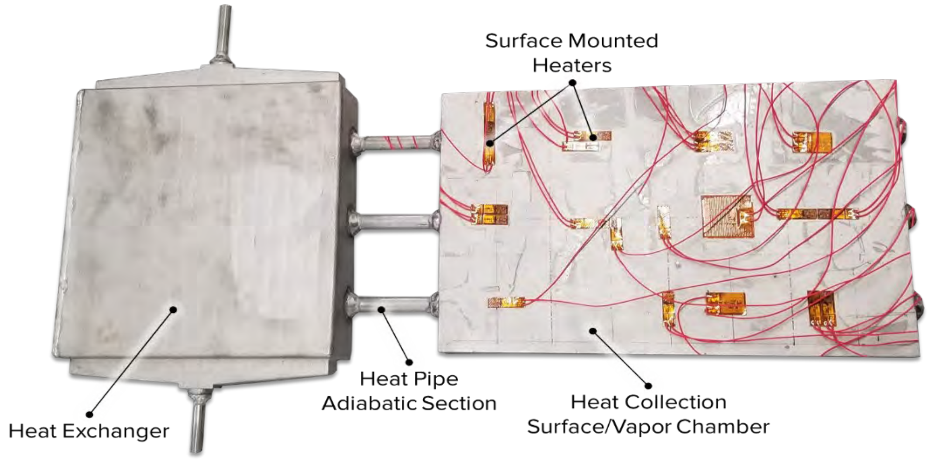

Figure 8. Subscale Acetone VCCP.

2. Subscale Ammonia VCCP Fabrication

The Subscale Ammonia VCCP (Figure 9) was fabricated through DMLS out of the aluminum alloy AlSi10MG. Both the Vapor Chamber and Heat Exchanger were additively manufactured separately, with their respective portions of the heat pipes embedded within. Similar to the Subscale Acetone VCCP, aluminum tubes were then used to connect the components, and additional tubes were also added as fill tubes for both the vapor chamber and the heat pipes. The prototype was then charged with ammonia for the vapor chamber, and ammonia and argon for each heat pipe.

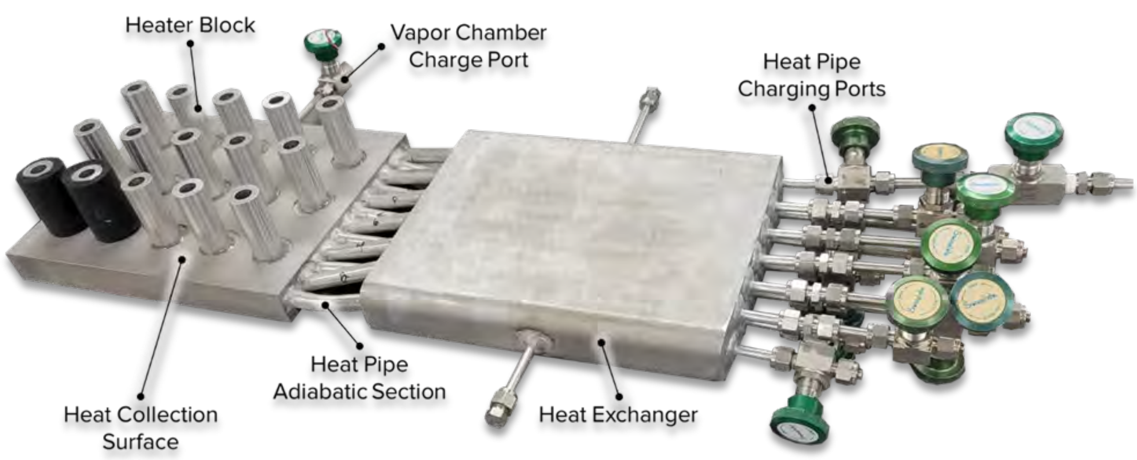

Figure 9. Subscale Ammonia Prototype VCCP.

3. Full-Scale VCCP Fabrication

The Full-Scale VCCP (Figure 10) was fabricated through traditional machining methods. Starting with the heat exchanger, an aluminum fin-tube assembly was fabricated, followed by an aluminum casing to surround the fins and heat pipe condenser portions. The evaporator portions of the aluminum heat pipes were then inserted into the aluminum vapor chamber. From there, the aluminum mesh was applied to the walls of the vapor chamber as well as the exterior walls of the heat pipes. Wicked connections were made to allow communication between the heat pipes and the heat collection surface of the vapor chamber. Finally, the vapor chamber was sealed with a lid, and charging ports for the vapor chamber and heat pipes were connected.

Figure 10. Full-Scale VCCP. The lid of the Vapor Chamber is removed in this image to provide an interior view.

B. Test Plan

To demonstrate the temporal isothermality of the VCCP prototypes, a test loop and program were constructed. Using a pumped single-phase loop (Figure 11), the coolant temperature was either increased or decreased at a steady rate. Thermocouples placed underneath the heat sources on the heat collection surface recorded the change in temperature of this surface, and the rate of change of this temperature was noted. To demonstrate the spatial isothermality of the VCCP prototypes, thermocouples were placed evenly across the heat collection surface. The heat load provided by the mounted heat sources was applied non-uniformly. This non-uniform heat load profile varied slightly by prototype but generally consisted of one heater powered up to a heat flux of 15.5 W/cm^2, with other heaters powered to either 5 or 10 W/cm^2, which was determined by the maximum power the cold plate was designed for. Temperature data collected across this surface could then be used to demonstrate the spatial isothermality provided by the vapor chamber.

At the time of this publication, testing had not been completed for the Full-Scale VCCP prototype.

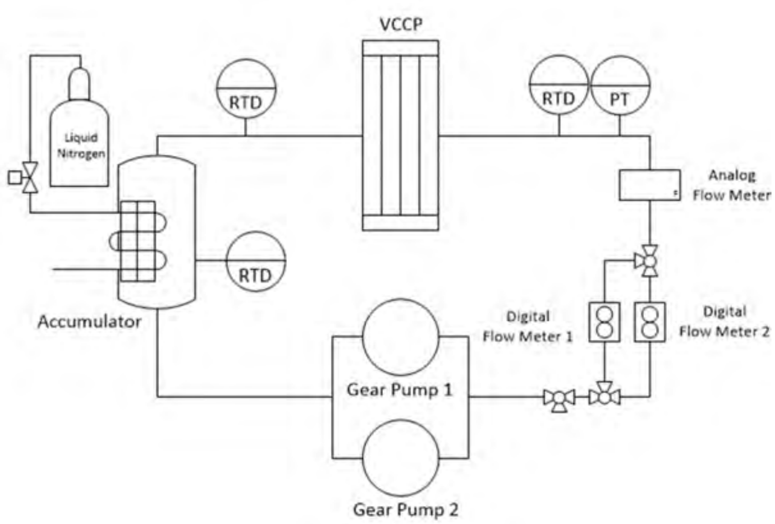

Figure 11. Test Loop.

C. Test Data

1. Subscale Acetone VCCP Testing Data

The test data for the Subscale Acetone VCCP was previously reported in ICES-2021-354 [1] but is included here for a comparison between this model and the Subscale Ammonia VCCP. A representative test showing the performance of the Subscale Acetone VCCP is shown in Figure 12. Note that the Phase I prototype was unable to demonstrate temporal isothermality, as the temperature of the cold plate was exceeding its safety temperature limit, causing the heaters to cycle on and off, preventing the system from reaching steady state conditions. However, the spatial temperature deviation was determined to be 2 K or less among the temperature measurements, showing good spatial isothermality.

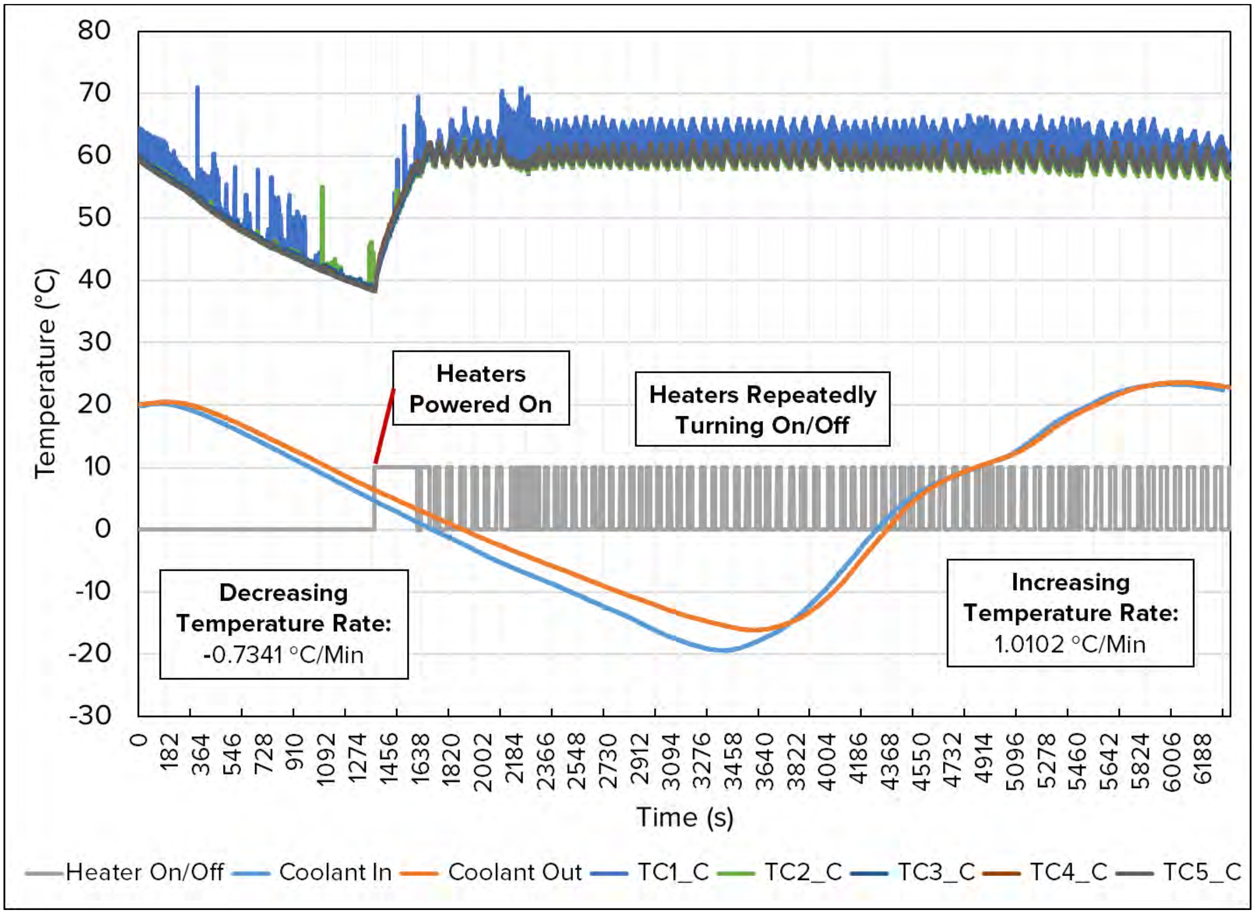

Figure 12. Representative Test of the Subscale Acetone VCCP, Temperature vs. Time.

2. Subscale Ammonia VCCP Testing Data

The Subscale Ammonia VCCP prototype was tested using the same test bed and testing parameters as were used for the Subscale Acetone VCCP prototype. However, cartridge heaters were used in place of pressure-activated adhesive resistive heaters, which enabled higher heat loads to be tested (up to 100 W per heater, resulting in heat fluxes of 15.5 W/in^2). These cartridge heaters were individually controlled, so a variety of non-uniform thermal loads could be applied. Additionally, only 15 thermocouples were used, in place of the 22 used for the Subscale Acetone VCCP. A representative graph demonstrating the performance of the Subscale Ammonia VCCP can be seen in Figure 13. This test shows how each temperature recorded across the surface of the VCCP changes as the coolant temperature changes. The rate of change for each highlighted section is described in Table 3.

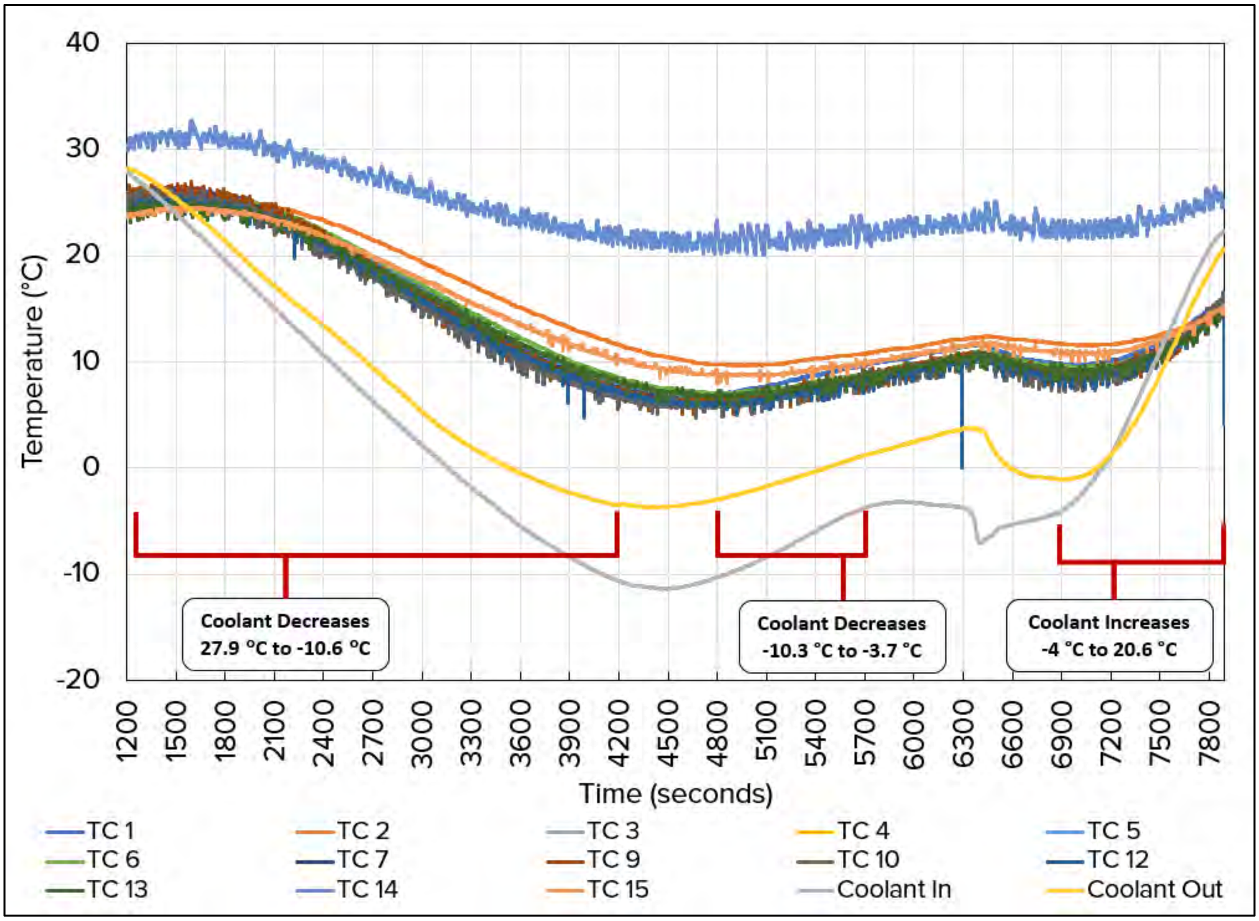

Figure 13. Representative Test of the Subscale Ammonia VCCP, with one Heater (captured by TC 14) powered to 24 W/cm²; Temperature vs. Time.

Table 3. Rates of Temperature Change for Subscale Ammonia VCCP; Tested with Single Heat Source Powered to 24 W/cm².

	Coolant Decrease from 27.9 °C to -10.6 °C	**Coolant Increase from -10.3 °C to -3.7 °C**	**Coolant Increase from -4 °C to -20.6 °C**
Coolant Temperature Rate of Change	-0.77 °C/min	0.43 °C/min	1.64 °C/min
Average Surface Temperature Rate of Change	-0.46 °C/min	0.17 °C/min	0.53 °C/min
Heat Source Temperature Rate of Change	-0.24 °C/min	0.3 °C/min	0.41 °C/min

3. Full-Scale VCCP Testing Data

While the Full-Scale VCCP was fully fabricated, the system was over-pressurized and was damaged as a result. As such, no testing data was collected for the Full-Scale VCCP.

IV. Conclusion

This research was performed as a part of a now-completed Phase II SBIR Program funded by NASA and summarizes the development of the VCCP technology across scales, both in terms of power load and in terms of size. In exploring the performance of the two subscale models, the Subscale Acetone VCCP which experienced the lowest thermal loads performed better than the Subscale Ammonia VCCP in terms of the spatial isothermality. However, the

Subscale Ammonia VCCP demonstrated adequate temporal isothermality despite rapidly changing sink conditions, as shown in Table 3. In this table, the coolant temperate changes as high as a rate of 1.65 °C/minute, yet at this rate the average surface temperature of the heat collection surface changes by 0.53 °C/minute. The temperature rate of change recorded directly underneath the heat source is even lower in this instance, 0.41 °C/minute, due to its proximity to the heat source.

This reduction in temperature rate of change experienced by the heat collection surface compared to the coolant temperature rate of change is beneficial for spacecraft which experience rapidly changing sink conditions such as Low-Earth Orbit (LEO) satellites. By reducing the temperature rate of change on the heat collection surface, the VCCP can improve the performance and extend the lifetime of temperature-sensitive mounted electronics.

We believe the VCCP technology has a self-imposed limitation, as it tries to reduce the area through which heat passes from that of the heat collection surface area down to the surface area of the heat pipes. In this way, the VCCP acts as a heat flux concentrator, and so the limiting factor of the technology becomes the limitations of the VCHPs. Therefore, any scaling limitations of the technology are also restricted by the limitations of the heat pipes within the cold plate. This limitation could be overcome by adjusting the evaporator geometry of the VCHPs from a circular cross-section to a flat design similar to the vapor chamber itself.

Acknowledgments

ACT acknowledges Aryiannah McGee and Max Demydovych for their efforts in data acquisition for this research. Additionally, ACT thanks the NASA SBIR program for financially supporting the development of the technology discussed here.

References

[1] M. C. Ellis and E. K. Seber, "Development of a Cold Plate for Spatial and Temporal Isothermality (ICES-2021-354)," in *International Conference on Environmental Systems*, 2021.